

## Biomat Effects On Wastewater Infiltration From Onsite System Dispersal Trenches

S.D. Finch and L.T. West  
University of Georgia

One of the primary factors that must be considered in evaluations of soil suitability for an onsite system drainfield, expected performance of various types of drainfield products, and different drainfield geometries is the rate at which wastewater will infiltrate into the soil from the trench. It is fairly easy with current technology to measure the saturated hydraulic conductivity ( $K_s$ ) of a soil. However, because the soil is receiving wastewater instead of clean water, the soil  $K_s$  decreases over time in response to dispersion, structure breakdown, and pore clogging from solid and organic loading. Thus, the challenge is to understand and eventually predict the decay in wastewater infiltration rate as the soil at the trench interface changes with wastewater additions. If this can be accomplished for the range in soil and climatic conditions, a long term acceptance rate can be derived from measured soil hydraulic data rather than being empirically estimated. Thus, the objective to this study was to evaluate the wastewater infiltration rate for trench bottoms and sidewalls of mature onsite systems in Georgia and to use this data to derive a  $K_s$  of the biomat formed at the soil-trench interface.

### Methods

Seven mature onsite systems were sampled in the Georgia Piedmont and Coastal Plain. At each site, triplicate undisturbed cores were collected from the trench bottom and sidewall at two or three locations in each drainfield. Corresponding vertically and horizontally-oriented core samples were collected from natural soils at the same depths that trench samples were collected. Core  $K_s$  was measured with the constant head method (Klute and Dirksen, 1986) using 0.1 M  $\text{CaCl}_2$  to prevent dispersion. After  $K_s$  measurement, undisturbed samples were collected from the cores, impregnated with epoxy resin containing a fluorescent additive, and polished blocks were prepared (Stoops, 2003). The polished blocks were photographed under ultraviolet light, and porosity (pores  $>0.05$  mm equivalent circular diameter) was evaluated by image analysis at 1 mm depth increments from the soil-trench interface. From these data, the base of the biomat was estimated to be the depth at which porosity increased to that of the natural soil.

Hydrus-2D was used to model two-dimensional water flows from trenches (Rassam et al., 2003). For the simulations, only one-half of the dispersal field was modeled since the two halves of the trench were assumed to be symmetrical. The dispersal field configuration used for model simulations was a 45 cm wide (half that of a full trench) and 31 cm deep trench with the water table 60 cm below the trench bottom. The trench was aggregate filled with a distribution pipe 22 cm from the trench bottom. The trench bottom and sidewall biomat thickness was 3 cm, with the sidewall biomat extending to a height of 11 cm above the trench bottom. Although measurements indicated the biomat in these soils was less than 0.8-cm thick, a biomat thickness of 3 cm was used for model simulations in order to increase the number of nodes within the biomat. The biomat  $K_s$  was increased from that measured at the sites such that the biomat hydraulic resistance was the same as that measured for the soil being simulated.

The flow (Q) per day through the trench bottom and trench sidewall was evaluated per cm trench length (units of  $\text{cm}^3 \text{cm}^{-1} \text{d}^{-1} = \text{cm}^2 \text{d}^{-1}$ ). The wastewater loading rate was  $2 \text{ cm d}^{-1}$  applied in three equal doses during the day at 0800 h, 1400 h, and 2000 h. Dosing times were chosen from the frequency pattern of a single-family residence (USEPA, 2002). Each dose lasted 48 minutes. The loading rates are typical loading rates used for soils with properties similar to these (USEPA, 2002).

Water retention parameters and hydraulic conductivity for the simulations were predicted using Hydrus-2D's neural network. Particle size distribution, bulk density, and  $K_s$  measured for the sites were input and van Genuchten's parameters ( $n$ ,  $\alpha$ ,  $\theta_s$ ,  $\theta_r$ ) were derived by the model. Aggregate in the trench had van Genuchten parameters and hydraulic conductivity that was representative of coarse material.

There were two model simulations. One simulation had the same  $K_s$  for the trench bottom and trench sidewall. The simulation assumed that the sidewall biomat  $K_s$  was twice that of the trench bottom. Model simulations were run until total outflow reached steady state, which required 13 d.

## Theory

Using Darcy's Law, hydraulic resistance (R) can be derived by solving for hydraulic flux (Eq. [1]) and  $\Delta H$  (Eq. [2]). Because current is analogous to hydraulic flux ( $J_w$ ) in Eq. [1] and voltage is analogous  $\Delta H$  (Eq. [1]), the hydraulic resistance (R) can be derived using Eq. [3].

$$J_w = \frac{Q}{A} = -K_s \times \left( \frac{\Delta H}{L} \right) \quad [1]$$

$$\Delta H = \frac{-J_w \times L}{K_s} \quad [2]$$

The soil's resistance can also be calculated by using soil length and  $K_s$  (Eq. [3]).

$$R = \frac{-\Delta H}{J_w} = \frac{L}{K_s} \quad [3]$$

The effective hydraulic resistance is the sum of the resistance of the soil layers (Eq. [4]). The effective saturated hydraulic conductivity ( $K_{eff}$ ) is calculated by solving Eq. [5].

$$R_{eff} = \sum_{z=1}^N R_z = \sum_{z=1}^N \frac{L_z}{K_z} = \frac{\sum_{z=1}^N L_z}{K_{eff}} \quad [4]$$

$$K_{eff} = \frac{\sum_{z=1}^N L_z}{\sum_{z=1}^N \frac{L_z}{K_z}}$$

[5]

By using the  $K_{eff}$  equation for the biomat affected soil (Eq. [6]), the  $K_s$  of the biomat ( $K_B$ ) can be calculated using Eq. [7] (White, 2002; White and West, 2003).

$$K_{eff} = \frac{L_B + L_N}{\frac{L_B}{K_B} + \frac{L_N}{K_N}}$$

[6]

$$K_B = \frac{L_B}{\left[ \frac{L_B + L_N}{K_{eff}} - \frac{L_N}{K_N} \right]}$$

[7]

$K_{eff}$ = $K_s$  measured on core samples

$L_B$ =thickness of the biomat from thin section polished block samples

$K_B$ = $K_s$  of biomat

$L_N$ =thickness of soil in core below biomat

$K_N$ = $K_s$  of natural soil and mean measurements taken from natural soil

## Results and Discussion

### Biomat Thickness

Visual estimates of biomat thickness in the field ranged from <1 to more than 30 mm (Figs. 1 and 2). Variability in thickness was due to differences in system age, wastewater loading rate, system design, and method of wastewater distribution for the systems sampled. In addition to variation among the drainfields, biomat thickness varied within the drainfields because of installation imperfections that resulted in uneven wastewater loading. Serial wastewater distribution within the drainfield also resulted in considerable differences in biomat thickness and hydraulic characteristics within drainfields as did unequal wastewater distribution because distribution boxes were not level and/or un-level trench bottoms.



Figure 1. Biomat from trench bottom. Thickness of dark material is about 3 cm.

Quantitative evaluations of biomat thickness from porosity evaluations with depth suggest that the dark color typically used to estimate biomat thickness at a macro scale may overestimate actual thickness of the zone with appreciable pore plugging. In samples with a thick dark-colored layer, the upper part of the darkened layer had low porosity as would be expected from pore infilling by organic materials (Figs. 2 and 3). The lower part of the darkened layer, however, was more porous suggesting the dark color in this layer was from staining of grain surfaces instead of pore infilling (Figs. 2 and 3).

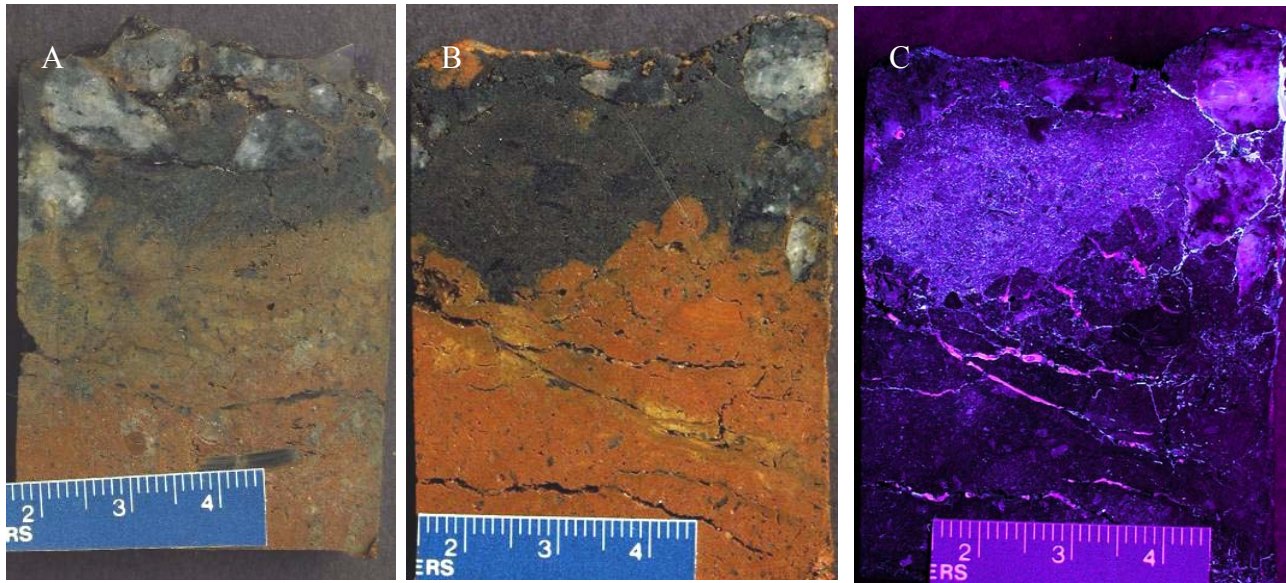


Figure 2. Trench bottom biomat samples; A – plane light image from Site C, B – plane light image from Site D, C – same view as B except photographed under UV light.

Porosity measurements by image analysis indicated that only the upper few mm of the wastewater impacted soil had reduced pore area (Fig. 3). In addition, the pore size in the clogged zone was appreciably less than the underlying soil. Biomat thickness ranged from 0.4 to 0.8 cm with an overall mean of 0.5 cm (Table 1). Similar thicknesses have been reported in other studies that quantitatively evaluated biomat thickness (Siegrist, 1987; Laak, 1970; Jones and Taylor, 1965) although thicker biomats have also been reported (Magdoff and Bouma, 1975).

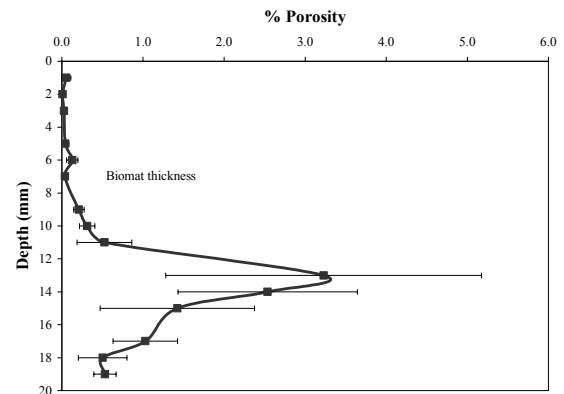


Figure 3. Percentage porosity with depth of polished block sample from Site C. The biomat was estimated to be 7 mm thick at this site.

Table 1. Biomat thickness of trench bottom and trench sidewall derived from the porosity measurements of polished block samples.

Site	Trench Bottom		Trench Sidewall		Mean
	Thickness	n	Thickness	n	Thickness
	cm		cm		cm
A	0.4(0.12) <sup>†</sup>	3	NA <sup>‡</sup>	NA	0.4(0.12)
B	0.4(0.10)	2	0.6(0.10)	2	0.5(0.08)
C	0.5(0.20)	2	0.7	1	0.6(0.13)
D	0.6(0.05)	2	0.6	1	0.6(0.03)
E	0.5(0.09)	7	0.3	1	0.5(0.08)
F	0.8(0.55)	2	NA	NA	0.8(0.55)
G	0.4(0.05)	10	NA	NA	0.4(0.05)
Total Mean	0.5(0.05)		0.6(0.07)		0.5(0.04)

<sup>†</sup> Standard error is in parenthesis.

<sup>‡</sup> Sidewall samples could not be sampled at Sites A and G because of chamber systems and the sidewall samples at Site F were damaged during polished block preparation.

The fabric and grain-size in the dark colored porous zone in the biomat sample from Site 4 was different from that of the subjacent soil and was similar to fabric expected for a sandy textured soil (Fig. 2C). This sandy fabric suggests that sand may have been placed in the trench bottom during drainfield construction. The homeowners, however, indicated that no sand had been added to the trench bottoms during installation. Thus, it is hypothesized that high organic loading and constant saturated or near-saturated and anoxic conditions induced chemical reduction of Fe and Mn at the soil-trench interface. One consequence of Fe and Mn reduction is generation of protons, and resulting acid conditions destroyed clay leaving the more resistant sand. The soil immediately underlying the biomat had colors that suggested that the soil was currently strongly reduced as indicated by bluish-gray color. Such modification of the soil may result in the soil having greatly different hydraulic properties than was measured or estimated at the time of onsite system installation.

There were no significant differences between vertical and horizontal  $K_s$  for natural soils or any significant difference between trench bottom and trench sidewall  $K_{eff}$ . Thus, only means for all samples of natural and biomat impacted soils at each site will be discussed. The  $K_s$  of natural vertical soils ranged from 0.0 (Site C) to 40 (Site G) cm/d and varied widely within and among sites (Table 2). The trench bottoms at Sites A – F were installed in soil horizons with loam to sandy clay textures, weak structure, and resulting low  $K_s$ . At a few of the sites, the horizon containing the drainfield also had weakly developed platy structure which further reduced the  $K_s$  of the natural soil at the sites. The low  $K_s$  for sites A – F suggest that these horizons were only marginally suitable for drainfield installation. None of the systems sampled, however, were in hydraulic failure.

The  $K_{eff}$  for biomat-affected soils was 0.1 to 2.9  $cm\ d^{-1}$  (Table 2). When comparing the natural soil (NS) and the biomat-affected soil (BS) within each site, the natural soil  $K_s$  was significantly higher than the biomat-affected soil at Sites A, C, and G (Table 2). Although the  $K_s$  and  $K_{eff}$  were significantly different in Site C, the  $K_s$  value for natural soil was less than the  $K_{eff}$  for the biomat-impacted soil. Site D did not show a statistical difference but the natural soil  $K_s$  was higher than the  $K_{eff}$  of the biomat-impacted soil. The lack of reduction in  $K_s$  because of biomat formation at Sites B, C, E, and F, is interpreted to be due to a number of reasons, including low

$K_s$  of the natural soils, natural variability in  $K_s$ , and variability in biomat development. Sampling active gravel-filled dispersal fields to obtain undisturbed samples was extremely tedious and minor disturbances may have occurred for part of the sample.

Table 2. Geometric mean of  $K_s$  of natural soil (NS) and  $K_{eff}$  of biomat-affected soil (BS), hydraulic resistance, and percent of K reduction from biomat formation.  $\alpha=0.10$

Site	Texture	NS	R of NS	BS	R of BS	K
		Mean $K_s$ cm d <sup>-1</sup>	d	Mean $K_{eff}$ cm d <sup>-1</sup>	d	Reduction %
A	cl	3.2(0.3) <sup>†</sup> a <sup>§</sup>	2.4	0.5(0.4)b	18.0	86
B	l	1.1(0.3)a	7.1	0.7(0.2)a	11.3	34
C	c	0.0(0.3)a	321.4	1.5(0.1)b	5.8	NA <sup>‡</sup>
D	sc	0.4(0.3)a	13.6	0.1(0.3)a	95.1	77
E	c	0.0(0.3)a	213.4	0.1(0.5)a	95.1	NA
F	scl	0.3(0.5)a	25.9	2.7(0.4)a	3.0	NA
G	s	41(0.1)a	0.2	2.9(0.2)b	2.3	93

<sup>†</sup> Standard error is in parenthesis.

<sup>‡</sup> Percent reduction could not be calculated because NS<BS.

<sup>§</sup> Sites with the same letter indicate no significant difference between the NS and BS within the site at  $\alpha=0.10$ .

The reductions of K due to biomat formation were lower in this study than that reported by other studies (Jones and Taylor, 1965; Siegrist, 1987). Siegrist (1987) measured in situ the hydraulic conductivity properties of a dispersal field located in silty clay loam textured soil. The saturated hydraulic conductivity of the natural soil was 241 cm d<sup>-1</sup> and dropped to <1.3 cm d<sup>-1</sup> (99.5%) due to soil clogging. Jones and Taylor (1965) measured the steady hydraulic conductivity rate, under continuous percolation for twenty weeks, of sand (coarse and fine) packed columns, overlain with gravel. The sand textured soil  $K_s$  ranged from 610 to 1951 cm d<sup>-1</sup> and reduced to 1.83 to 7.32 cm d<sup>-1</sup> after biomat formation or 0.30 to 0.34% of the natural  $K_s$ . Lower percentage reduction of  $K_s$  due to biomat formation in this study, as compared to that reported by others, was interpreted because of lower  $K_s$  of the natural soils. For Site G, which had a sand texture, the  $K_s$  reduction due to biomat formation was 93%.

The hydraulic resistance for the natural soil of Sites A, B, D, and G ranged from 0.2 to 13.6 d, while the hydraulic resistance of the biomat-affected soil at these sites ranged from 2.3 to 95.1 d (Table 2). As the natural soil  $K_s$  decreased, the hydraulic resistance of biomat-affected soil increased. The hydraulic resistance of Magdoff and Bouma's (1975) sand textured soil with a biomat was 5.1 d, which is within the range of the biomat-affected soil's hydraulic resistance in this study. The hydraulic resistance of the natural soils at Sites C, E, and F ranged from 25.9 to 321.4 d, while the biomat-affected soil's hydraulic resistance ranged from 3.0 to 95.1 d (Table 2). Because remaining sites did not have reduced  $K_s$  values, the hydraulic resistances of the biomat-affected soil did not increase; however, the range of hydraulic resistance was similar to the other sites (Sites A, B, D, and G).

### Biomat $K_s$

Using the measured biomat thickness, thickness of natural soil in core samples, and  $K_{\text{eff}}$  of biomat impacted soils, and  $K_s$  of the natural soils, biomat  $K_s$  was calculated using Eq. [7]. The mean  $K_s$  of the biomat at Sites A, B, D, and G was 0.02, 0.12, 0.01, and 0.20  $\text{cm d}^{-1}$ , respectively. Hydraulic resistance of the biomat was 15.6, 4.3, 81.5, and 2.2 d for Sites A, B, D, and G, respectively (Table 3). Biomat  $K_s$  values reported by Keys et al. (1998) ranged from 0.02  $\text{cm d}^{-1}$  for the bottom and sidewall areas to 2.41  $\text{cm d}^{-1}$  for the unaffected upper sidewall. The biomat  $K_s$  values calculated in this study were within the  $K_s$  range reported by Keys et al. (1998).

Table 3. Hydraulic resistance and  $K_s$  of the biomat for sites that had measurable reduction in  $K$  due to biomat impact.

Site	R of biomat d	Biomat $K_s$ $\text{cm d}^{-1}$
A	15.6	0.02
B	4.3	0.12
D	81.5	0.01
G	2.2	0.20

### Model Simulations

The total trench output for the clay loam soil with equal trench bottom and trench sidewall biomat  $K_s$  was  $88.5 \text{ cm}^3 \text{ cm}^{-2} \text{ d}^{-1}$  which was 98.3% of the total input of  $90 \text{ cm d}^{-1}$  (Table 4-2). Ponding depths at steady state were 10.3, 10.9, and 11.2 cm for the dosing times at 0800 h, 1400 h, and 2000 h, respectively. The minimum ponding depth prior to the 0800 h dose was 9.4 cm; thus, flow through the trench bottom varied only slightly due to increased head associated with each dose (Fig. 4). Most of the variation in total outflow due to each dose application was from differences in sidewall flow (Fig. 4).

The majority of the flow,  $62.0 \text{ cm}^3 \text{ cm}^{-2} \text{ d}^{-1}$  (68.9%), was through the trench bottom, while  $26.5 \text{ cm}^3 \text{ cm}^{-2} \text{ d}^{-1}$  (29.4%) was through the trench sidewall (Fig. 4 and Table 4). The flow through biomat-affected sidewall was  $14.5 \text{ cm}^3 \text{ cm}^{-2} \text{ d}^{-1}$  (16.1% of the total flow), while the flow above the biomat was  $12.0 \text{ cm}^3 \text{ cm}^{-2} \text{ d}^{-1}$  (13.3%) (Table 4). Most of the increased sidewall flow associated with dose application was through natural soil above the biomat-impacted sidewall (Figs. 4 and 5). Sidewall flow above the biomat, reported by Keys et al. (1998), for a sand textured soil was  $2.41 \text{ cm d}^{-1}$ . This value is much higher than the flow acceptance in this study ( $0.27 \text{ cm d}^{-1}$ ), which was expected since the soil in this study had higher clay content and lower permeability. As ponding height decreased between doses, simulated flow continued in the zone just above the biomat although wastewater ponding height is below the top of the sidewall biomat. This flow may also be an artifact of the characteristics of the simulated media filling the trench. This artifact would not be expected to appreciably affect relative total daily flow through the trench bottom and sidewall, however.

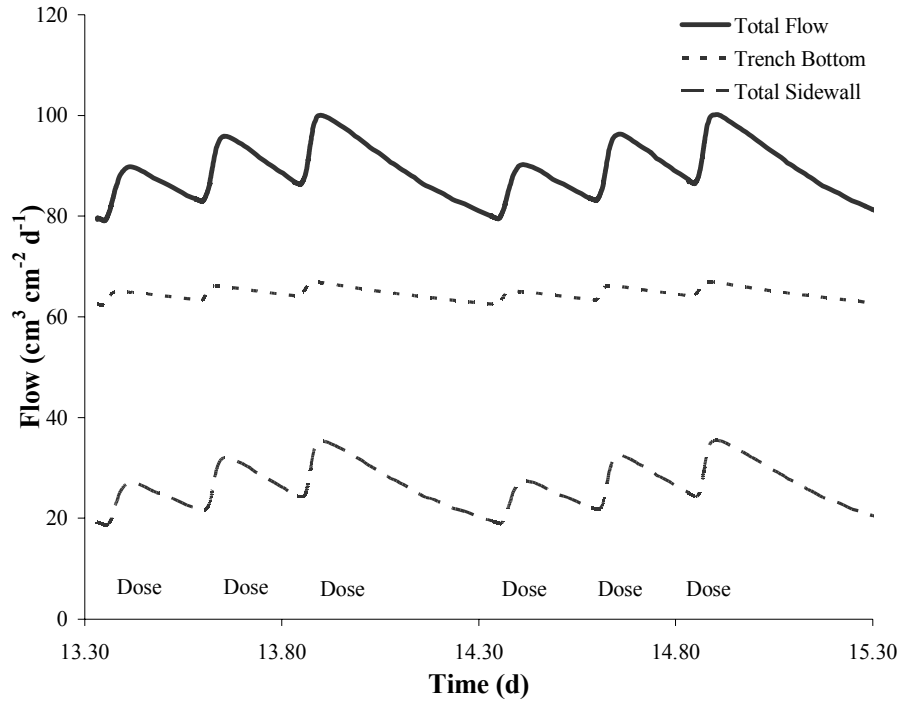


Figure 4. Total system, trench bottom, and sidewall flow of dispersal field in clay loam soil with equal trench bottom and sidewall  $K_s$ .

The clay loam system with the biomat sidewall  $K_s$  2 times greater than the bottom biomat  $K_s$  had a total outflow of  $88.0 \text{ cm}^3 \text{ cm}^{-2} \text{ d}^{-1}$  which was 97.8% of total inflow (Fig. 5 and Table 4). A majority of flow,  $60.0 \text{ cm}^3 \text{ cm}^{-2} \text{ d}^{-1}$  (66.7%), was through the trench bottom and the remaining flow,  $28.0 \text{ cm}^3 \text{ cm}^{-2} \text{ d}^{-1}$  (31.1%), was through the trench sidewall. The higher percentage of flow through the sidewall as compared to the simulation with equal trench bottom and trench sidewall biomat  $K_s$ , which was expected since the biomat affected sidewall was more permeable. The maximum ponding depths were 9.4, 9.9, and 10.3 cm for the daily doses (Fig. 5). Because ponding never reached 11 cm, there was no flow above the sidewall with biomat. Although sidewall flow increased, trench bottom flow for this simulation was only 2.2% less than was observed for the simulation where trench bottom and sidewall biomat  $K_s$  were equal.

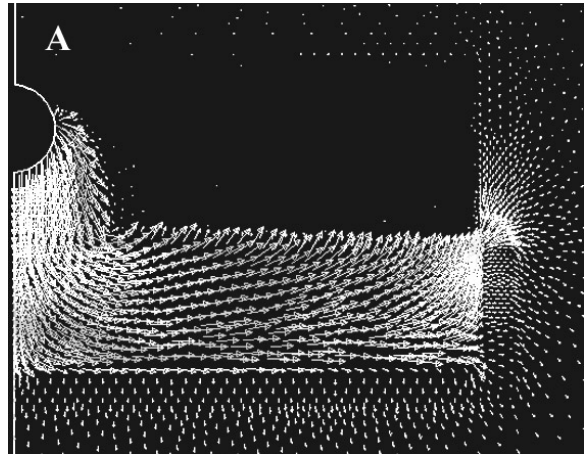


Figure 5. Velocity vectors for dispersal field in clay loam soil with equal  $K_s$  values for trench bottom and sidewall biomat.

Table 4. Calculated flows from model simulations.

K <sub>s</sub> trench sidewall versus bottom	Top	Sidewall with biomat	Total Sidewall	Trench Bottom	Input Flow	Output Flow
equal	0.5	14.5	26.5	62.0	90	88.5
sidewall=2*TB	0.5	28.0	28.0	60.0	90	88.0

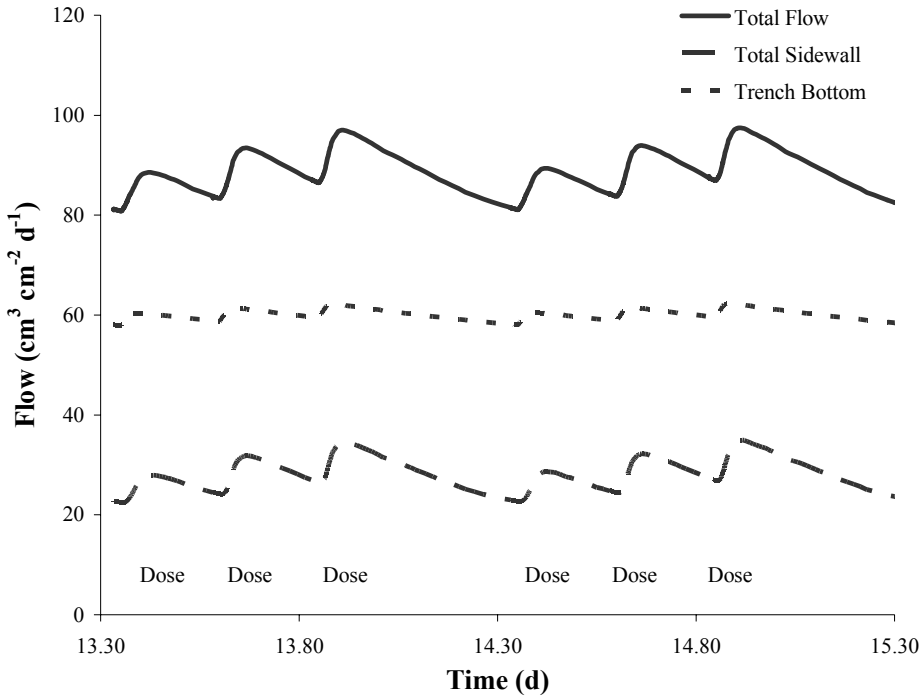


Figure 6. Total system flow, sidewall flow, and trench bottom flow of dispersal field in clay loam soil with 2 times the trench sidewall biomat K<sub>s</sub> than the trench bottom biomat K<sub>s</sub>.

### Conclusions

The K<sub>s</sub> of the natural vertical and horizontally oriented soil samples were not statistically different and ranged from 0.0 to 41 cm d<sup>-1</sup>. The biomat-affected soil taken from the trench sidewall and bottom were also not statistically different. The K<sub>eff</sub> of the biomat-affected soil ranged from 0.2 to 2.9 cm d<sup>-1</sup>. Reduction in K<sub>s</sub> from biomat formation was observed at four of the seven sites, with the reduction ranging from 34 to 93% of the natural soil K<sub>s</sub>. The lack of reduction at the remaining sites was interpreted to be due to low K<sub>s</sub> of the natural soil, natural variability in K<sub>s</sub>, and variability in biomat development because of system design, system age, system installation, wastewater loading rates, and wastewater distribution.

Visual estimates of the biomat thickness ranged from <0.1 to >3 cm; however, biomat thicknesses ranged from 0.4 to 0.8 cm after quantitative measurements were made using fluorescence microscopy. Calculated biomat K<sub>s</sub> ranged from 0.02 to 0.20 cm d<sup>-1</sup> for Sites A, B, D, and G with hydraulic resistance ranging from 2.2 to 81.5 d.

For the model simulations with equal trench sidewall and bottom  $K_s$  and with trench sidewall  $K_s$  being 2 times greater the trench bottom  $K_s$ , there was higher trench bottom flow (66.7 to 68.9%) than sidewall flow (29.4 to 31.1%). When the simulated biomat having a  $K_s$  twice that to the trench bottom biomat, ponding height decreased and sidewall flow occurred only through the biomat-affected sidewall.

## References

- Jones, J.H. and G.S. Taylor. 1965. Septic tank effluent percolation through sands under laboratory conditions. Soil Sci. The Williams and Wilkins Co., USA.
- Keys, J.R., E.J. Tyler, and J.C. Converse. 1998. Predicting life for wastewater absorption systems. p. 167-176. *In Proc. of the Eighth Natl. Symp. on Individual and Small Community Sewage Systems*, 8<sup>th</sup>, Orlando, FL, USA. 8-10 Mar. 1998. ASAE Publ. 10-91:192-200. St. Joseph, MI.
- Klute, A. and C. Dirksen. 1986. Hydraulic conductivity and diffusivity: Laboratory methods. p. 687-734. *In A. Klute (ed.) Methods of soil analysis. Part 1. 2nd ed. Agron. Monogr. 9* ASA and SSSA, Madison, WI.
- Laak, R. 1970. Influence of domestic wastewater pretreatment on soil clogging. *J. Water Pollut. Control Fed. Part I.* 42:1495-1500.
- Magdoff, F. R. and J. Bouma. 1975. The development of soil clogging in sands leached with septic tank effluent. p. 37-47 *In Proc. of the Natl. Home Sewage Disposal Symp.* ASAE Publ. Chicago, USA. 9-10 Dec. 1974. St. Joseph, MI.
- Rassam, D., J. Šimůnek, and M.Th. van Genuchten. 2003. Modeling variably saturated flow with hydrdrus-2d. ND Consult. Brisbane, Australia.
- Siegrist, R.L. 1987. Soil clogging during subsurface wastewater infiltration as affected by effluent composition and loading rate. *J. Environ. Qual.* 16:181-187.
- Stoops, G. 2003. Guidelines for analysis and description of soil and regolith thin sections. SSSA, Inc. Madison, WI, USA.
- USEPA. 2002. On-site wastewater treatment systems manual. EPA/625/R-00/008 Office of Water. Office of Research and Development. (Available on-line <http://www.epa.gov/ORD/NRMRL/Pubs/625R00008/625R00008.pdf>.) (Verified 13 Aug. 2002.)
- White, K.D. 2002. Evaluation of the hydraulic conductivity of EZ flow brand hardened expanded polystyrene aggregate as compared to gravel systems. [Online].
- White, K.D. and L.T. West. 2003. In-ground dispersal of wastewater effluent: The science of getting water into the ground. *Small Flows Quarterly*.